Gold Atoms Promote Macroscopic Superconductivity in an Atomic Monolayer of Pb on Si(111)

Denis S Baranov, Sergio Vlaic, Jonathan Baptista, Enrico Cofler, Vasily Stolyarov, Dimitri Roditchev, Stéphane Pons

Gold atoms promote macroscopic superconductivity in an atomic monolayer of Pb on Si(111)

Denis S. Baranov,[†,‡,¶] Sergio Vlaic,[†] Jonathan Baptista,[†] Enrico Cofler,[§] Vasily Stolyarov,[‡,¶] Dimitri Roditchev,[†,‖] and Stéphane Pons[*,†]

†*Laboratoire de Physique et d'Étude des Matériaux (LPEM), ESPCI Paris, Université PSL, CNRS UMR8213, Sorbonne Université, 75005 Paris, France*

‡*Moscow Institute of Physics and Technology (State University), Dolgoprudny, Moscow 141700, Russia*

¶*Institute of Solid State Physics, Russian Academy of Sciences, Chernogolovka, Moscow 142432, Russia*

§*Laboratoire de Physique et d'Étude des Matériaux, ESPCI Paris, Université PSL, CNRS UMR8213, Sorbonne Université, 75005 Paris, France*

‖*Institut des Nanosciences de Paris, Sorbonne Université, CNRS UMR7588, 75005 Paris, France*

E-mail: stephane.pons@espci.fr

Phone: +33 1 40 794 575

Abstract

Atomically thin superconductivity in Pb-monolayers grown on Si(111) is affected by adding a tiny amount of Au-atoms. In-situ macroscopic electron transport measurements reveal that superconductivity develops at higher temperatures and manifests a sharper superconducting transition to zero-resistance as compared to pristine Pb/Si(111). Scanning tunneling microscopy and spectroscopy show that Au atoms decorate atomic step

edges of Pb/Si(111) and link the electronic reservoirs of neighbouring atomic terraces. The propagation of superconducting correlations across the edges is enhanced facilitating the coherence between terraces and promoting macroscopic superconductivity at higher temperature. This finding opens new ways to design and control Josephson junctions at the atomic scale.

Keywords

Monolayer Semiconductor, Proximity Effect, Superconducting transition, Electrical conductivity, Scanning tunneling microscopy

Introduction

The use of superconducting materials is one of the most promising strategies for the development of quantum technologies.[1,2] The interest for the superconducting behaviour at nanoscale raised with the wish to decrease the size of superconducting devices. However, because of size and geometry or the influence of local defects and the environment, many phenomena can impact the superconducting coherent quantum state in small superconductors such as phase fluctuations and quantum confinement. Also, low dimensional superconductors are prone to the interplay with other quantum ground states such as magnetism or charge ordering. All these phenomena can hinder the superconducting transition or alter transport properties and the efficiency of quantum devices. In 3D systems, for instance, the Anderson criterion which limits the minimal size for the emergence of superconductivity by the electronic level spacing was found robust and cannot be overcome.[3] In 2D materials however, superconductivity was discovered to subsist at the ultimate thicknesses of a single atomic layers.[4–7] However, in low dimensional systems the screening of structural and chemical defects occurs at large distance. As a consequence defects may have a dramatic effect on the emergence of macroscopic superconducting order.[6] For example, atomic step edges in atomic superconductors have been shown to behave as sharp potential barriers for Cooper pairs which dis-

rupt the continuity of the electronic system and convert it in a percolating Josephson network.[6,8,9] Therefore, defects such as step edges are weak points for superconductivity in that case.[6,10–12] Here we show that by decorating the step edges of a superconducting Pb/Si(111) monolayer with a tiny amount of gold atoms yields a strong coupling of the superconducting terraces and turn these weak points into strong links.

Results

Scanning tunneling microscopy results

Two kinds of samples were prepared following the procedure described in Ref.[13] (see methods section for details). Our reference sample was made of a single atomic layer of Pb deposited on Si(111) and the other ones were made of Au-containing Pb/Si(111). As we show below, it enables stabilizing atomically ordered dense Pb/Si(111) identical to Au-free reference samples but with step edges decorated by Au atoms.

Figure 1 displays constant current topographic scanning tunneling microscopy (STM) images of the reference sample Pb/Si(111) (a) and of Au-containing Pb/Si(111) surface (b). The reconstruction of Pb on atomic terraces is quite similar in both cases. The reconstruction of Pb on atomic terraces is quite similar in both cases and shows a very specific topographic patterns where small domains present 3 lateral protrusions. It corresponds to the well-recognized striped incommensurate structure (SIC)[4,6,14] of Pb/Si(111); The ideal SIC contains 1.33 monolayers (ML) of Pb on top of a Si(111) substrate atoms, with 1 ML denoting a 100% coverage with Pb pseudomorphic to Si(111). The topography patterns are then induced by the fact that there are more atoms in the surface layer than in the substrate underlying plane.[4,14] In some rare locations elsewhere in the surface,[13] more linear phases for which Pb atom density corresponding to coverage of around 1.30 monolayer[15] are found. It denotes very low-density fluctuation of Pb atoms in the surface layer. Atomic terraces in Au-Pb/Si(111) are small with characteristic radius of the order of 20-50nm (see supporting information and ref.[13]) whereas SIC-Pb/Si(111) exhibits larger (200nm) and

elongated terraces.[6] The step edge structures of the two samples of figure 1a) and b) are obviously different; in Au-Pb/Si(111) samples the step termination at surface equilibrium is made of a double of Au atoms.[13]

The scanning tunneling spectroscopy (STS) also revealed significant differences in the local density of states (DOS) of the samples, as seen in figure 1c). On terraces, the tunneling conductance spectra $dI/dV(V)$ of both systems are quite identical (grey and pink lines in figure 1c)). The rise of the conductance below -300 mV (above +800 mV) is related to the contribution of the valence (conductance) bands of silicon. Both spectra are characterized by a low DOS at the Fermi level, as expected for the Pb interface states with the Fermi level located in the band gap of silicon. From these data it is evident that Au atoms do not play a significant role in the structural organization of the layer of the Pb stripe incommensurate structure over the terrace nor on its electronic properties, but the situation changes dramatically at the step edges. Indeed, the tunneling data acquired at the step edge of the reference sample (black curve) differs significantly from the one acquired at the Au-decorated step edge (red curve). Precisely, the tunneling spectrum at Au-decorated edge exhibits an additional spectral feature at -400 mV (a second smeared feature is also visible at +300 mV) and a higher DOS at the Fermi level (zero-bias).

Transport properties

Electron transport measurements were achieved by using 4-contacts directly in the STM head using a miniature homemade probe which was gently landed on the surface (see figure 2a) and methods section). The soft landing of the 4 contacts causes only very limited damages on the surface, as revealed in ex-situ scanning electron microscopy images, figure 2b). The results of transport experiments are presented in figure 2c).

For both systems, $R(T)$ exhibits a plateau before the transition to the superconducting state. At the plateau, the absolute value of R is slightly higher for the reference Pb/Si(111) sample, probably reflecting a higher in-series resistance of atomic edges. In this sample, the plateau in $R(T)$ lasts down to approximately 3.0 K, in agreement with previous work.[5] Below, the resistance

starts to decrease progressively, with an almost linear $R(T)$ observed below 2.0 K. In this sample zero-resistance was not reached even at 1.15 K. On the contrary, in Au-Pb/Si(111), the onset of the superconducting transition is observed already at 4.5 K witnessing the extended range of superconducting fluctuation regime. As the temperature is further lowered, the $R(T)$ dynamics accelerates. Finally, the resistance vanishes at $T_c^t \approx 1.25$ K. The sheet resistance of the sample is close to the quantum resistance which makes the sample prone to superconducting fluctuations. The measurements evidence stronger superconducting fluctuations than expected by a two-dimensional Aslamasov-Larkin and Maki-Thompson model[5] (see supporting information). Note that the overall shape of $R(T)$ is robust; it was reproduced in several locations of each studied sample. It was also verified that, the injection current do not perturbs the measurements up to $1\ \mu A$ (see supporting information).

Proximity effect through Au-decorated step edges

We performed a local study of the propagation of superconducting correlations across the step edges of Au-Pb/Si(111) at 1.3-1.35 K when the sample is still not in a macroscopic superconducting state. A straightforward way to do it is put the sample in contact with a good superconductor and use the latter as a source of Cooper pairs.[16,17] At the interface with a non-superconducting system, Cooper pairs convert to Andreev quasiparticles[18] which propagate in the non-superconducting matter and carry a specific spectral footprint - a depletion in the quasiparticle DOS around the Fermi level, often referred to as a "proximity gap". The energy width of this proximity gap reflects the local strength of superconducting correlations. In non-superconducting metals, the proximity gap rapidly decreases as the STM tip is moved away from the interface and disappears,[19] usually on a scale of a few nanometers to a micrometer depending first on the coherence length of the Cooper pairs (i.e. the nature of the superconductor) and the temperature, the nature of the metal and of the interface, the structural quality and impurity density. This superconducting proximity effect was already spatially resolved in the vicinity of superconductor-normal metal interfaces[20–25] and around the vortex cores.[26] The proximity phenomenon can be extended to the case of a contact

between two superconductors with different superconducting gaps. In the vicinity of the contact, Cooper pairs propagate from one superconductor to the other and modify superconducting properties which can be measured in STS experiments.[27]

In the present case, small superconducting Pb-islands typical radius and thickness: 100 nm and 2 to 5 nm respectively) dispersed at the surface of our Au-Pb/Si(111) (seen on SEM picture in figure 2c)) were used as a source of Cooper pairs. The results of the study are summarized in figure 3. We have used a superconducting tip made of Pb/Ir for a better energetic resolution of the STS data (see methods section). Figure 3a) shows a topographic STM image on which the contrast of a single Pb-island appears saturated. The black arrow reproduces the trajectory followed by the STM tip when 810 local $I(V)$ tunneling spectra were acquired every 1 Å. The profile of the sample surface along the path is shown in figure 3b). The tip moved from Pb-island (region 1) to the first Pb/Si(111) terrace (region 2), crossed the step edge (region 3) and ended up on the second Pb/Si(111) terrace (region 4). Raw STS data ($dI/dV(V)$ spectra taken with a superconducting tip) are derived from experimental $I(V)$ curves and are presented in color scale in figure 3c) as a function of lateral position of the tip. They show a strong depletion around zero-bias (appearing in blue color). The depletion is due to the convolution of a superconducting gap of the tip with density of state of the sample. Figure 3d) presents the same results as in (c) but after suppressing the effect of the tip DOS and temperature (see methods and reference[28]). These data represent the DOS of the sample and display how the superconducting correlations (in blue) evolves. It becomes immediately clear that the transition from a large superconducting gap (region 1) into the proximity gap (region 2) occurs at a very short scale of a few nanometers. This jump is a sign of a low electron transparency between Pb-island and first Pb/Si(111) terrace. As the tip is moved away from Pb-island, the energy width of the proximity gap smoothly decreases. This is clear from figure 3e) where the evolution of the gap width (in meV) is plotted as a function of distance. Note that at temperature 1.35 K of the STS experiment, the sample is very close to full superconducting state. In this condition, superconducting correlations in the terraces are due to fluctuating Cooper pairs in Pb/Si(111) and superconducting correlations injected from the Pb island[27] and one can expect

that the superconducting decay to be large. The key feature is observed around the interface 3 between regions 2 and 4. While the tip moves from one atomic terrace to the other and crosses Au-decorated step, the proximity gap continues its smooth decrease showing no sign of reflection or disruption of the superconducting correlations across the Au-decorated step edge. This behavior is at variance with what has been observed in Pb/Si(111) genuine samples where step edges are weak links[6,27] causing an abrupt variation superconducting properties.[6,10] Our findings are consistent with macroscopic transport data and confirms the hypothesis that Au-decorated atomic step edges are highly transparent for superconducting correlations.

Conclusion

Scanning Tunneling Microscopy and Spectroscopy and macroscopic electron transport were used as complementary approaches to elucidate the role of Au-atoms which are decorating the step edges in atomically thin Pb/Si(111) superconductor. STS studies demonstrate that the superconducting correlations propagate across Au-decorated atomic steps without disruption suggesting that in Au-Pb/Si(111) superconducting terraces are much more strongly coupled together than in pure Pb/Si(111). This result is corroborated by transport measurements which show firstly a macroscopic superconducting transition at a higher T_c in Au-Pb/Si(111) than in Pb/Si(111), and secondly, a superconducting fluctuation regime extending to significantly higher temperatures in Au-Pb/Si(111). The strong coupling through steps decorated by Au-atoms could be due to the substantial increase of DOS at step edges or related to spin-momentum locking[29] mechanism since strong Rashba spin-orbit interaction was already evidenced in Au-chains on Si(111) surfaces.[30] Our work shows that the specific decoration of the steps, grain boundaries or other atomic-scale defects could be used for influencing macroscopic superconducting characteristics of two-dimensional superconductors. Our findings could also be extended to control Josephson junctions at the atomic scale.

Methods

Samples were prepared under ultrahigh vacuum (base pressure 1.1×10^{-10} mbar) just before their in-situ local and global studies. P-doped (6.3×10^{14} cm^{-3}) Si(111)-oriented wafers were used as substrates. The silicon surface was prepared by repeated direct current heating cycles consisting of flashes at 1150 °C. The last flashes were followed by slow cooling (-3 K/s) through the $1 \times 1 \rightarrow 7 \times 7$ reconstruction phase transition. The preparation procedure was repeated until the substrate exhibited ∼100 nm large atomically flat 7×7-Si(111) terraces, with typical in-antiphase chevron patterns at neighboring step edges. Any further annealing was achieved by radiative heating. Dense atomic ML of Pb/Si(111) were obtained by electron beam assisted deposition of 1.3 ML of Pb at a rate of approximately 0.33 ML/min on 7×7-Si(111) held at room temperature (RT). After deposition, the samples were annealed at 370 ° C for 15 minutes. Au-Pb samples were prepared with successive depositions of Au and Pb. 0.6 ML of gold was first deposited by MBE at a rate of 0.2 ML/min on Si(111) at RT. The 5×2 crystallographic order was obtained by annealing the sample 2 min at 580 ° C. The sample was then annealed at 420 °C for 15 min to stabilize the similar Pb reconstructions on the terraces as pure Pb/Si(111) sample but with step edges decorated by Au atoms.[13]

Four-terminal probes consist of four soft Au-wires of 10 μm in diameter separated by 20 to 50 μm from each other, see figure 2a). The wires are fixed on a ceramic support using an electrically insulating glue. The probe can be moved laterally thanks to the piezoelectric actuators of the microscope, thus reaching different regions of the sample. The extremity of each Au-wire is bend to form a soft spring; the spring heights are adjusted in such a way that during the probe approach the wires land successively on the surface of the sample. Upon landing, the quality of each contact is monitored, thanks to the current amplifier of the microscope, from tunneling to ohmic contact regimes. Once the first contact is reached, the probe is further moved remotely using the step-by-step regime of the piezoelectric approach motor of STM until all the probes reach ohmic contacts to the surface.

Four-terminal measurements were performed using a Keithley 2400 current source and a Keith-

ley 2182 nanovoltmeter. To suppress eventual contribution from thermopower sources, for each data point the DC-current was set in one direction (I_+), and the voltage drop δV_+ measured. The direction of DC-current was then inverted ($I_- = -I_+$) and the corresponding voltage drop δV_- was measured. The resistance R was calculated as follows:

$$R = \frac{\delta V_+ - \delta V_-}{I_+ - I_-} \tag{1}$$

The sample temperature was piloted by a LakeShore 336 controller using a Cernox® sensor and a resistive heater integrated into the STM sample stage. The lowest temperature of 1.15 K was achieved using the Joule-Thomson refrigerator of the microscope cryostat in the "single-shot" regime. This base temperature remains fixed for up to 2 hours (until Joule-Thomson pot becomes empty), and then rises to 4 K. An additional resistive heating allows for extending the accessible temperature range to 30-40 K. From STM experiments we know that in the studied temperature range the thermal drift of the junction in lateral and vertical directions does not overcome a few nm. From SEM data in figure 2c) one can indeed see that the probe motion in the landing area occurs at a scale much shorter than the distance between neighbouring Au-wires, insuring that unperturbed large sample area are probed during transport measurements.

STM/STS measurements were achieved in-situ in ultrahigh vacuum by means of a "Tyto SPM" from SPECS™ at a base temperature of 1.3 K; the tunneling bias was applied to the sample. Superconducting Pt/Ir tips covered with a thick layer of Pb were used. The use of Pb covered tip allows us to take advantage of the sharp quasiparticle peaks at the edges of the superconducting gap to improve the energy energetic resolution in spectroscopy, usually limited in metallic tips by thermal broadening to $\sim 3.5k_BT$.[31] The required deconvolution of the spectroscopic data followed the procedure Ref.[28] Reference spectra acquired in-situ on bulk-like Pb islands enabled establishing a precise shape of the superconducting spectrum of each used tip. All the tips were characterized by a superconducting density of states and critical temperature similar to bulk Pb. Topographic figures were prepared by means of WsXM software.[32] The analysis of the STM/STS data was done with

homemade Mathematica and Python procedures.

Supporting Information

Supporting information is available free of charge via the internet at http://pubs.acs.org.

Large scale topography image, comparison of the experimental data with two-dimensional Aslamasov-Larkin and Maki-Thompson model, evolution of the electrical resistance with the injection current.

Acknowledgement

SP acknowledges Brigitte Leridon for useful discussion. The authors thank the French national research agency for the support of the SUPERSTRIPES project, Ref. ANR-15-CE30-0026. Tip production and transport measurements were partially supported by grant No. 21-72-00148 from the Russian Science Foundation. The PhD grant of J.B. was supported by the Labex Matisse (Sorbonne University) and the Nexans Chair of the ESPCI-Paris Georges Charpak Endowment Fund through the PhaseOnSi project. The PhD work of D.B. was supported by Vernadskii grant from French Ministry of Foreign Affairs.

References

(1) Devoret, M. H.; Schoelkopf, R. J. Superconducting Circuits for Quantum Information: An Outlook. Science **2013**, 339, 1169–1174.

(2) Arute, F. et al. Quantum supremacy using a programmable superconducting processor. Nature **2019**, 574, 505–510.

(3) Vlaic, S.; Pons, S.; Zhang, T.; Assouline, A.; Zimmers, A.; David, C.; Rodary, G.; Girard, J.-

C.; Roditchev, D.; Aubin, H. Superconducting parity effect across the Anderson limit. Nature Communications **2017**, 8, 14549.

(4) Zhang, T.; Cheng, P.; Li, W.-J.; Sun, Y.-J.; Wang, G.; Zhu, X.-G.; He, K.; Wang, L.; Ma, X.; Chen, X.; Wang, Y.; Liu, Y.; Lin, H.-Q.; Jia, J.-F.; Xue, Q.-K. Superconductivity in one-atomic-layer metal films grown on Si(111). Nature Physics **2010**, 6, 104–108.

(5) Yamada, M.; Hirahara, T.; Hasegawa, S. Magnetoresistance Measurements of a Superconducting Surface State of In-Induced and Pb-Induced Structures on Si(111). Phys. Rev. Lett. **2013**, 110, 237001.

(6) Brun, C.; Cren, T.; Cherkez, V.; Debontridder, F.; Pons, S.; Fokin, D.; Tringides, M. C.; Bozhko, S.; Ioffe, L. B.; Altshuler, B. L.; Roditchev, D. Remarkable effects of disorder on superconductivity of single atomic layers of lead on silicon. Nature Physics **2014**, 10, 444–450.

(7) Wu, X.; Ming, F.; Smith, T. S.; Liu, G.; Ye, F.; Wang, K.; Johnston, S.; Weitering, H. H. Superconductivity in a Hole-Doped Mott-Insulating Triangular Adatom Layer on a Silicon Surface. Phys. Rev. Lett. **2020**, 125, 117001.

(8) Yoshizawa, S.; Kim, H.; Kawakami, T.; Nagai, Y.; Nakayama, T.; Hu, X.; Hasegawa, Y.; Uchihashi, T. Imaging Josephson Vortices on the Surface Superconductor $\mathrm{Si}(111)-(\sqrt{7}\times\sqrt{3})-\mathrm{In}$ using a Scanning Tunneling Microscope. Phys. Rev. Lett. **2014**, 113, 247004.

(9) Uchihashi, T.; Mishra, P.; Aono, M.; Nakayama, T. Macroscopic Superconducting Current through a Silicon Surface Reconstruction with Indium Adatoms: $\mathrm{Si}(111)-(\sqrt{7}\times\sqrt{3})-\mathrm{In}$. Phys. Rev. Lett. **2011**, 107, 207001.

(10) Kim, H.; Lin, S.-Z.; Graf, M. J.; Miyata, Y.; Nagai, Y.; Kato, T.; Hasegawa, Y. Electrical Conductivity through a Single Atomic Step Measured with the Proximity-Induced Superconducting Pair Correlation. Phys. Rev. Lett. **2016**, 117, 116802.

(11) Howon Kim, Y. M.; Hasegawa, Y. Superconducting proximity effect on a Rashba-split Pb/Ge(111)-3 × 3 surface. Supercond. Sci. Technol. **2016**, 29, 084006.

(12) Oguro, F.; Sato, Y.; Asakawa, K.; Haze, M.; Hasegawa, Y. Enhanced critical magnetic field for monoatomic-layer superconductor by Josephson junction steps. Phys. Rev. B **2021**, 103, 085416.

(13) Baptista, J.; Vlaic, S.; Cofler, E.; Roditchev, D.; Pons, S. Stabilization of dense metallic Pb monolayer by decorating step edges with Au atoms on Si(111). Surface Science **2021**, 712, 121887.

(14) Hupalo, M.; Schmalian, J.; Tringides, M. C. "Devil's Staircase" in $\mathrm{Pb/Si(111)}$ Ordered Phases. Phys. Rev. Lett. **2003**, 90, 216106.

(15) Stepanovsky, S.; Yakes, M.; Yeh, V.; Hupalo, M.; Tringides, M. The dense -3×3Pb/Si(111) phase: A comprehensive STM and SPA-LEED study of ordering, phase transitions and interactions. Surface Science **2006**, 600, 1417 – 1430.

(16) De Gennes, P. G. Boundary Effects in Superconductors. Rev. Mod. Phys. **1964**, 36, 225–237.

(17) Deutscher, G.; de Gennes, P. In Superconductivity; Parks, R., Ed.; Marcel Dekker, Inc.: New York, 1969; Vol. 1; pp 1005–1034.

(18) Andreev, A. F. Thermal conductivity of the intermediate state of the superconductors. Soviet Physics JETP **1964**, 19, 1.

(19) Pannetier, B.; Courtois, H. Andreev Reflection and Proximity effect. Journal of Low Temperature Physics **2000**, 118, 599–615.

(20) Vinet, M.; Chapelier, C.; Lefloch, F. Spatially resolved spectroscopy on superconducting proximity nanostructures. Phys. Rev. B **2001**, 63, 165420.

(21) Escoffier, W.; Chapelier, C.; Hadacek, N.; Villégier, J.-C. Anomalous Proximity Effect in an Inhomogeneous Disordered Superconductor. Phys. Rev. Lett. **2004**, 93, 217005.

(22) le Sueur, H.; Joyez, P.; Pothier, H.; Urbina, C.; Esteve, D. Phase Controlled Superconducting Proximity Effect Probed by Tunneling Spectroscopy. Phys. Rev. Lett. **2008**, 100, 197002.

(23) Kim, J.; Chua, V.; Fiete, G. A.; Nam, H.; MacDonald, A. H.; Shih, C.-K. Visualization of geometric influences on proximity effects in heterogeneous superconductor thin films. Nature Phys. **2012**, 8, 464–469.

(24) Serrier-Garcia, L.; Cuevas, J. C.; Cren, T.; Brun, C.; Cherkez, V.; Debontridder, F.; Fokin, D.; Bergeret, F. S.; Roditchev, D. Scanning Tunneling Spectroscopy Study of the Proximity Effect in a Disordered Two-Dimensional Metal. Phys. Rev. Lett. **2013**, 110, 157003.

(25) Natterer, F. D.; Ha, J.; Baek, H.; Zhang, D.; Cullen, W. G.; Zhitenev, N. B.; Kuk, Y.; Stroscio, J. A. Scanning tunneling spectroscopy of proximity superconductivity in epitaxial multilayer graphene. Phys. Rev. B **2016**, 93, 045406.

(26) Stolyarov, V. S.; Cren, T.; Brun, C.; Golovchanskiy, I. A.; Skryabina, O. V.; Kasatonov, D. I.; Khapaev, M. M.; Kupriyanov, M. Y.; Golubov, A. A.; Roditchev, D. Expansion of a superconducting vortex core into a diffusive metal. Nature Communications **2018**, 9, 2277.

(27) Cherkez, V.; Cuevas, J. C.; Brun, C.; Cren, T.; Ménard, G.; Debontridder, F.; Stolyarov, V. S.; Roditchev, D. Proximity Effect between Two Superconductors Spatially Resolved by Scanning Tunneling Spectroscopy. Phys. Rev. X **2014**, 4, 011033.

(28) Pillet, J.-D.; Quay, C. H. L.; Morfin, P.; Bena, C.; Yeyati, A. L.; Joyez, P. Andreev bound states in supercurrent-carrying carbon nanotubes revealed. Nature Physics **2010**, 6, 965–969.

(29) Yoshizawa, S.; Kobayashi, T.; Nakata, Y.; Yaji, K.; Yokota, K.; Komori, F.; Shin, S.; Sakamoto, K.; Uchihashi, T. Atomic-layer Rashba-type superconductor protected by dynamic spin-momentum locking. Nature Communications **2021**, 12, 1462.

(30) Barke, I.; Zheng, F.; Rügheimer, T. K.; Himpsel, F. J. Experimental Evidence for Spin-Split Bands in a One-Dimensional Chain Structure. Phys. Rev. Lett. **2006**, 97, 226405.

(31) Pan, S. H.; Hudson, E. W.; Davis, J. C. Vacuum tunneling of superconducting quasiparticles from atomically sharp scanning tunneling microscope tips. Applied Physics Letters **1998**, 73, 2992–2994.

(32) Horcas, I.; Fernández, R.; Gómez-Rodríguez, J. M.; Colchero, J.; Gómez-Herrero, J.; Baro, A. M. WSXM: A software for scanning probe microscopy and a tool for nanotechnology. Review of Scientific Instruments **2007**, 78, 013705.

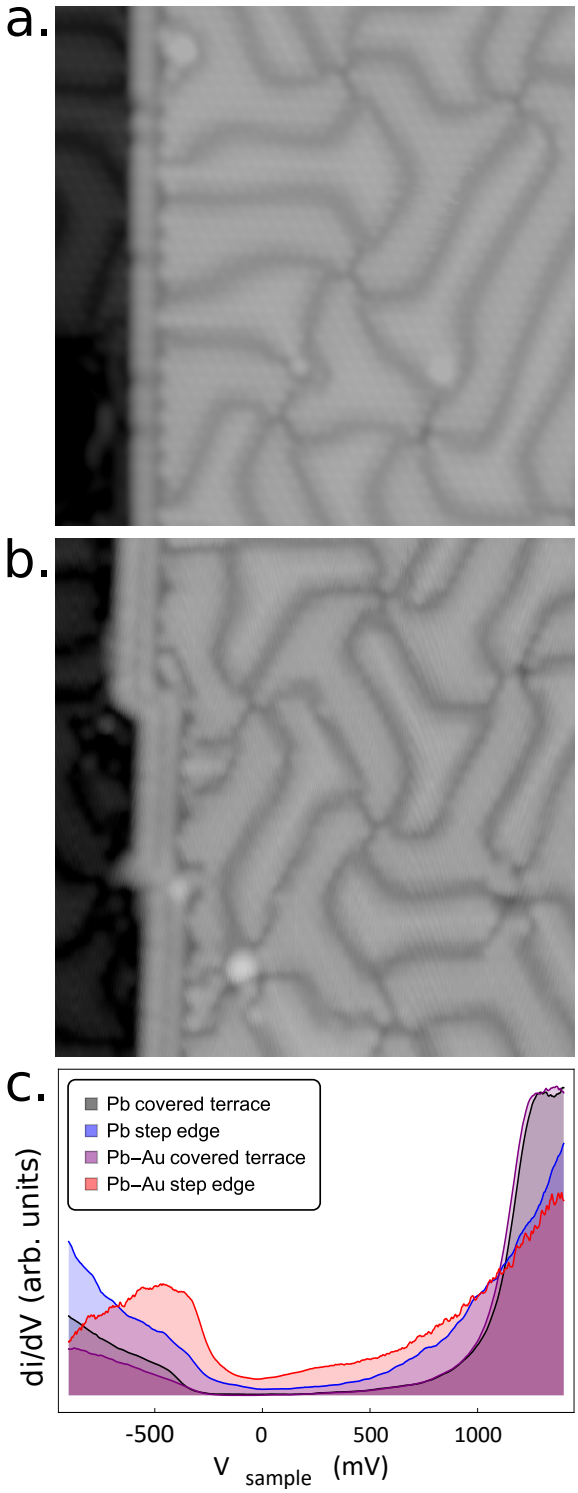

Figure 1: **Structure and electronic properties of Au-Pb/Si(111).** **a** - constant current (V_{bias}= 1.5 V, I= 50 pA) $25 \times 25\,\mathrm{nm}^2$ topographic STM image of the surface of stripe incommensurate structure (SIC) of Pb/Si(111) reference sample. Two atomic terraces separated by Pb-decorated step edge are seen. **b** - $25 \times 25\,\mathrm{nm}^2$ STM image of Au-Pb/Si(111) surface. Step edge is decorated by a double-row of Au-atoms and the terraces are covered by the stripe incommensurate structure of Pb. **c** - spatially averaged local tunneling conductance $dI/dV(V)$ spectra taken on terraces and step edges of images (a) and (b). Stabilization parameters: V_{bias}= 1.5 V and I= 50 pA.

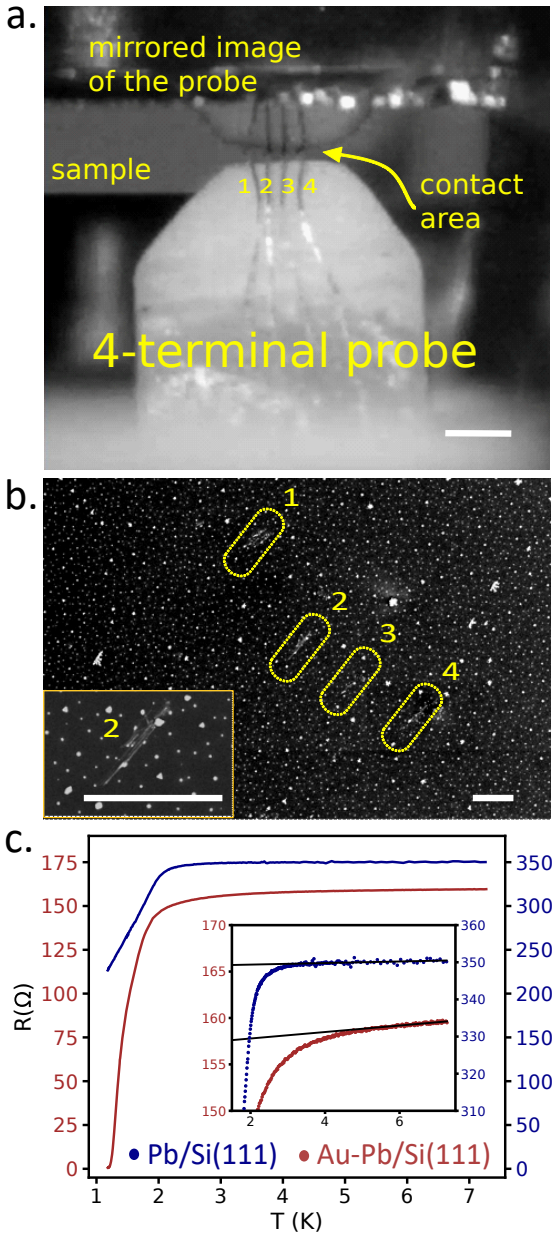

Figure 2: **Four-terminal probe and in-situ transport measurements.** **a** - picture of the probe mounted in the STM head and approached to the sample. Extremities of four $10\,\mu m$ thick Au-wires are bend to form soft springs reaching electric contacts with the sample surface. Scale bar $= 500\,\mu m$. **b** - SEM image ex-situ of the sample after transport and STM measurements. Numbers mark tiny scratches produced by corresponding contacts during landing of gold wires. The surface shows also nano-crystals of Pb dispersed on the surface. Inset: zoom on the area of one Au-contact landing. Scale bars = $25\,\mu m$. **c** - temperature evolution of resistance in the vicinity of superconducting transition for Pb/Si(111) (blue) and Au-Pb/Si(111) (red) samples. For both measurements, the transport current $I = 0.5\,\mu A$. **inset** zoom around the departure from the linear regime. In Pb/Si(111) the onset of the superconducting transition takes place at $\sim$3 K, whereas it transits at $\sim$4.5 K in Au-Pb/Si(111) samples (see supporting information). The resistance disappears at T_c=1.23 K in Au-Pb/Si(111); in Pb/Si(111) the zero-resistance state was not reached down to 1.15 K.

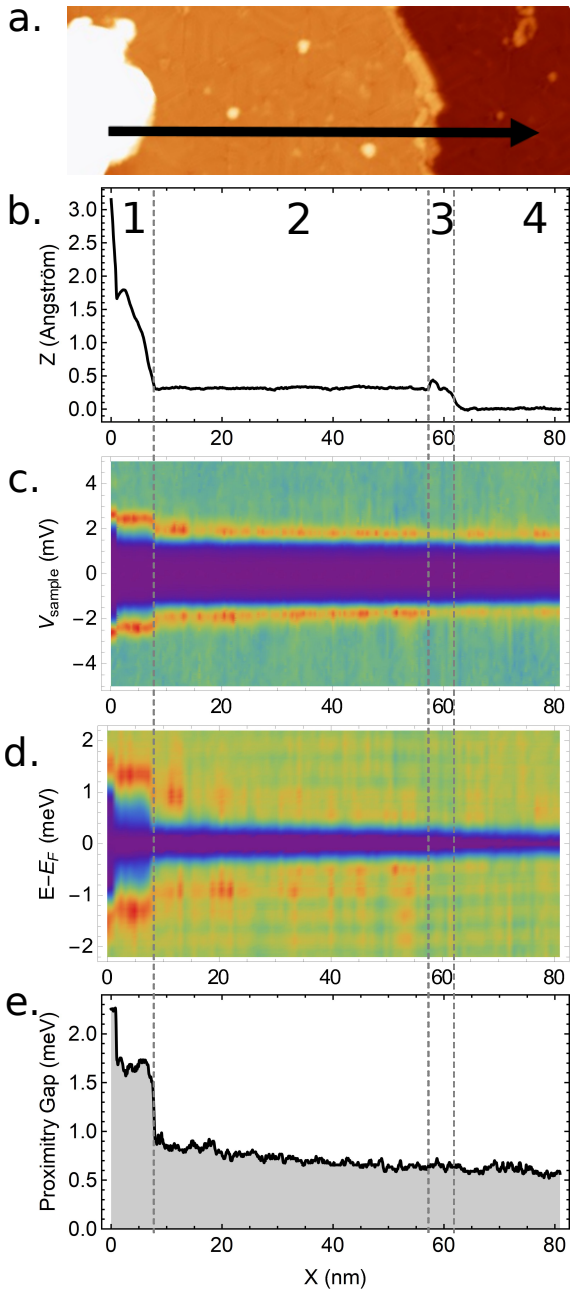

Figure 3: **Propagation of superconducting correlations in Au-Pb/Si(111).** **a** - $90 \times 30\text{nm}^2$ topographic STM image of the studied region (I=20 pA, V_{bias}=225 mV). Selected Pb-nano-island appears in white; the arrow marks the trajectory of the tip during STS. **b** - line cut of the topography along the STS trajectory. Regions: 1 - corresponds to the position of superconducting Pb island; 2 - to first stripe incommensurate structure (SIC) of Pb/Si(111) terrace; 3 - to step edge decorated with Au-atoms; 4 - to second SIC-Pb/Si(111) terrace. **c** - tunneling conductance spectra taken with a superconducting Pb/PtIr tip all along the trajectory following the arrow in (a). Stabilization parameters: V_{bias}=6 mV, I=20 pA. **d** - tunneling DOS of the sample deconvoluted from data in (c) following Ref.[28] **e** - evolution of the proximity gap energy extracted from (d) along the tip path. With increasing the distance from Pb-island, it exhibits a smooth decay and crosses the atomic step (region 3) without discontinuity.

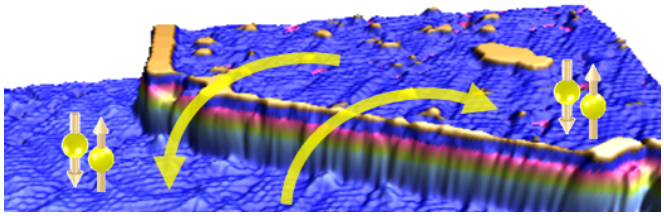

Table of Content Graphics